Microsc. Microanal. 10, 647–655, 2004
DOI: 10.1017/S1431927604040887

Microscopy AND Microanalysis

Acidocalcisomes of *Phytomonas françai* Possess Distinct Morphological Characteristics and Contain Iron

Kildare Miranda,[1,2] Claudia O. Rodrigues,[2] Joachim Hentchel,[3] Anibal Vercesi,[2,4] Helmut Plattner,[3] Wanderley de Souza,[1] and Roberto Docampo[2,*]

[1]*Laboratório de Ultraestrutura Celular Hertha Meyer, Instituto de Biofísica Carlos Chagas Filho, Universidade Federal do Rio de Janeiro, Av. Brigadeiro Trompovski, s/n., bloco G, Cidade Universitária, 21949-900, Rio de Janeiro, RJ, Brazil*
[2]*Laboratory of Molecular Parasitology, Department of Pathobiology and Center for Zoonoses Research, University of Illinois at Urbana–Champaign, Urbana, IL 61802*
[3]*Department of Biology, University of Konstanz, 78457 Konstanz, Germany*
[4]*Laboratório de Bioenergética, Núcleo de Medicina e Cirugia Experimental, Universidade Estadual Campinas, Campinas-SP, Brazil*

Abstract: Acidocalcisomes are acidic calcium storage compartments described initially in trypanosomatid and apicomplexan parasites, and recently found in other unicellular eukaryotes. The aim of this study was to identify the presence of acidocalcisomes in the plant trypanosomatid *Phytomonas françai*. Electron-dense organelles of *P. françai* were shown to contain large amounts of oxygen, sodium, magnesium, phosphorus, potassium, calcium, iron, and zinc as determined by X-ray microanalysis, either *in situ* or when purified using iodixanol gradient centrifugation or by elemental mapping. The presence of iron is not common in other acidocalcisomes. *In situ*, but not when purified, these organelles showed an elongated shape differing from previously described acidocalcisomes. However, these organelles also possessed a vacuolar H^+-pyrophosphatase (V-H^+-PPase) as determined by biochemical methods and by immunofluorescence microscopy using antibodies against the enzyme. Together, these results suggest that the electron-dense organelles of *P. françai* are homologous to the acidocalcisomes described in other trypanosomatids, although with distinct morphology and elemental content.

Key words: *Phytomonas*, acidocalcisomes, elemental mapping, pyrophosphatase, calcium, transmission electron microscopy

Introduction

Infection of plants with trypanosomatids was shown as early as 1909, when Lafont (1909) described the presence of flagellate protozoa in lactiferous plants. Plant trypanosomatids include those that live in the latex of various families of lacticiferous plants, in the phloem vessels of palms, coffee trees, and other plants, in the fruit sap and seeds of several plant families, and in flowers (Catarino et al., 2001). Most of them occur as promastigotes and a few as choanomastigotes and are transmitted to their plant hosts by phytophagous insects. It has been generally considered that parasites found in lactiferous tubes are not pathogenic. One exception is *Phytomonas françai*, which infects cassava (*Manihot esculenta*), a plant of economic interest, inducing the poor development of its root system and chlorosis of aerial parts (Kitajima et al., 1986). In addition, some species of intraphloematic trypanosomatids are important plant pathogens, causing diseases such as phloem necrosis in coffee (Stahel, 1931; Vermeulen, 1963), heart rot in coconut (Parthasarathy et al., 1976) and sudden wilt in oil palm (Dollet et al., 1977), and are responsible for the destruction of many plantations in Central and South America (Camargo, 1999).

Protozoan parasites can cause diseases that affect millions of people, animals (Anonymous, 1997), and plants (Camargo, 1999) worldwide, leading to great social and economic losses. The current chemotherapy against these parasites faces many problems that include low specificity and/or high toxicity of the drugs used and drug resistance. Therefore, it is important to search for biochemical targets that could be used for rational development of improved therapies. The understanding of the mechanisms involved in the control of Ca^{2+} homeostasis in parasitic protozoa has gained attention in recent years (for reviews, see Benaim, 1996; Docampo & Moreno, 1996). Cell viability requires perfect functioning of these mechanisms, and disruption of Ca^{2+} homeostasis by toxins can lead to cell death (Berridge,

Received March 15, 2003; accepted May 6, 2003.
*Corresponding author. E-mail: rodoc@staff.uiuc.edu

1997). In addition, Ca^{2+} is known to be involved in the invasion of host cells by different parasites, a process that is crucial for maintaining their life cycles (Moreno et al., 1994; Lu et al., 1997; Vieira & Moreno, 2000).

Previous studies concerning Ca^{2+} homeostasis in trypanosomatids have demonstrated that most of these cells have three intracellular Ca^{2+} pools that comprise the endoplasmic reticulum, mitochondria, and acidocalcisomes (Docampo & Vercesi, 1989*a*, 1989*b*; Vercesi et al., 1991*a*,*b*; Docampo & Moreno, 1999, 2001). Mitochondrial Ca^{2+} uptake occurs by an electrophoretic mechanism, is inhibited by antimycin A, FCCP and ruthenium red, and is stimulated by respiratory substrates, phosphate and acetate. This pool has a high capacity and a low affinity for Ca^{2+} and is able to buffer external Ca^{2+} at concentrations in the range of 0.6–0.7 μM, as occurs with vertebrate mitochondria (Docampo & Vercesi, 1989*a*, 1989*b*). Ca^{2+} uptake by the endoplasmic reticulum occurs via a Ca^{2+}-ATPase and is inhibited by high concentrations of vanadate and anticalmodulin agents. This pool has a low capacity and a high affinity for Ca^{2+} and is able to buffer external Ca^{2+} at concentrations in the range of 0.05–0.1 μM (Vercesi et al., 1991*b*). Acidocalcisomes are acidic vacuoles that contain a considerable fraction of intracellular Ca^{2+}, which can be released by nigericin, a K^+/H^+ ionophore, via alkalinization of the interior of the vacuole (Vercesi et al., 1994; Docampo et al., 1995). They possess a vacuolar-type H^+-ATPase and/or a vacuolar H^+-pyrophosphatase for proton uptake, a Ca^{2+}/H^+ countertransporting ATPase for Ca^{2+} uptake, and a Ca^{2+}/nH^+ antiporter for Ca^{2+} release (Docampo & Moreno, 1999, 2001). A Na^+/H^+ antiporter that may participate in Ca^{2+} release from these organelles has also been described in *Trypanosoma brucei* (Vercesi & Docampo, 1996, Vercesi et al., 1997; Rodrigues et al., 1999*a*) and *L. donovani* (Vercesi et al. 2000).

In this work, we provide evidence for the presence of acidocalcisomes in the plant trypanosomatid *Phytomonas françai*. These acidocalcisomes are morphologically different, although functionally similar, to acidocalcisomes of other trypanosomatids, being characterized by their high iron content and elongated shape *in situ*.

Materials and Methods

Cell Cultures

Promastigotes of *P. françai* isolated from cassava (Vainstein & Roitman, 1985) were grown in Warren's medium (Warren, 1960) at 28°C supplemented with 10% (v/v) heat inactivated fetal bovine serum. At 2–3 days after inoculation, cells were collected by centrifugation and washed twice in 250 mM sucrose (for TEM preparations) or in Dulbecco's phosphate buffered saline (PBS). Cells were suspended in Dulbecco's PBS for cell fractionation and physiological assays. Protein was determined by using the Bio-Rad Coomassie blue method.

Chemicals

Dulbecco's PBS, ethylene glycol-bis(β-aminoethyl ether)-N,N,N′,N′-tetraacetic acid (EGTA), 2-hydroxyethyl-1-piperazineethanesulfonic acid (HEPES), protease inhibitors, and nigericin were purchased from Sigma Chemical Company (St. Louis, MO). Acridine orange (AO) was obtained from Molecular Probes (Eugene, OR). Polyclonal antibodies raised against a keyhole limpet hemocyanin-conjugated synthetic peptide corresponding to the hydrophilic loop XII (antibody PAB_{HK} or 326) of plant V-H^+-PPase (Zhen et al., 1997) and aminomethylenediphosphonate (AMDP) (Zhen et al., 1994) were kindly provided by Prof. Philip Rea, University of Pennsylvania (Philadelphia, PA). All other reagents were of analytical grade.

Conventional Transmission Electron Microscopy

Cells were washed in Dulbecco's PBS, pH 7.2, fixed in 2.5% glutaraldehyde, 4% paraformadehyde in 0.1 M cacodylic acid buffer, postfixed in 1% OsO_4 plus 0.8% ferrocyanide and 5 mM $CaCl_2$ in 0.1 M cacodylic acid buffer for 30 min, dehydrated in acetone series, and embedded in Polibed 812 epoxide resin. Sections of 70 nm were obtained and stained for 40 min in 5% aqueous uranyl acetate and for 5 min in lead citrate. Observation was made in a Zeiss 900 transmission electron microscope operating at 80 kV.

Imaging of Unfixed Whole Cells

Cells were washed and resuspended in 250 mM sucrose. Drops were applied to 200 mesh formvar/carbon-coated copper grids, allowed to adhere for 10 min, carefully blotted dry, and observed in an energy-filtering LEO EM 912 transmission electron microscope operating at 120 kV. Electron spectroscopic images were recorded at an energy loss of 60 eV using a spectrometer slit width of 20 eV.

Electron-Probe X-Ray Microanalysis

Energy-dispersive X-ray spectra were recorded from the acidocalcisomes present in whole cells adhered to formvar/carbon-coated copper grids. As control, spectra were collected from regions of the cytoplasm adjacent to acidocalcisomes and from formvar/carbon film. Specimens were analyzed in a LEO-912 transmission electron microscope operating at 80 kV. X rays were collected for 300 s using a Si(Li) detector with an ultrathin window in a 0–10-keV energy range with a resolution of 10 eV/channel. Analyses were performed using an Oxford Link ISIS system attached to the microscope.

Elemental Mapping

X-ray mappings were acquired in a LEO 912 Omega equipped with a scanning device. The microscope was operated at 80 kV using a tungsten filament, in the scanning transmission (STEM) imaging mode, spot size was 40 nm, and emission current ~10 μA. X rays were collected by a Li-drifted Si-detector (front area 30 mm^2) equipped with an ATW atmospheric window. Analyses were performed using a Link multichannel energy analyzer and Link ISIS 3.00 software (Oxford Instruments, Wiesbaden, Germany).

Immunofluorescence Microscopy

Cells fixed in freshly prepared 4% formaldehyde were allowed to adhere to poly(L-lysine)-coated coverslips, permeabilized with 0.3% Triton X-100 for 3 min, and blocked with 50 mM ammonium chloride and 3% bovine serum albumin in PBS. Immunofluorescence was carried out using a 1:100 dilution of anti-V-H^+-PPase antibody and a fluorescein isothiocyanate-coupled goat anti-rabbit IgG secondary antibody (1:100). Fluorescence images were obtained with an Olympus BX-60 fluorescence microscope fitted with a 493-nm excitation filter, a CCD camera, and an image analysis system.

Isolation of Electron-Dense Organelles

Electron-dense organelles were isolated by the iodixanol method similar to that described before for the isolation of acidocalcisomes of *Trypanosoma cruzi* (Scott & Docampo, 2000). Cells were washed twice with PBS, pH 7.2, and suspended in lysis buffer (20 mM HEPES, pH 7.2, 50 mM KCl, 125 mM sucrose, 0.5 mM ethylene diamine tetraacetic acid (EDTA), 5 mM dithiothreitol, 0.1 mM 4-(2-aminoethyl)benzenesulphonyl fluoride, 10 μM pepstatin A, 10 μM leupeptin, and 10 μM E-64). Cell pellets of *Phytomonas* were mixed with approximately 2× wet weight silicon carbide (Aldrich) and ground with a pestle and mortar until cell lysis reached 90%. The lysate was subsequently suspended in lysis buffer and centrifuged 10 min at 580 × *g* to remove the silicon carbide, unbroken cells, and debris. The supernatant was centrifuged for 10 min at 15,000 × *g*, and the pellet obtained was suspended in 4 ml of lysis buffer with the aid of a 22-gauge needle and applied to a discontinuous gradient of iodixanol, with 4-ml steps of 24, 28, 34, 37, and 40% iodixanol diluted in lysis buffer. The gradient was centrifuged at 50,000 × *g* in a Beckman SW 28 rotor for 60 min. The resulting fractions were suspended in lysis buffer and used in physiological assays. The fraction pelleted on the bottom of the tube was also used for electron microscopy preparations.

Proton Pump Activity

Pyrophosphate-driven proton transport was assayed by measuring changes in the absorbance of acridine orange (A_{493}-A_{530}) in an SLM-Aminco DW 2000 dual wavelength spectrophotometer. Cells were incubated at 30°C in 2.5 ml 130 mM KCl standard reaction medium containing in addition 2 mM $MgSO_4$, 10 mM HEPES, 50 μM EGTA, 1 μM oligomycin, 100 μM sodium pyrophosphate, 3 μM acridine orange, and different inhibitors where indicated. Each experiment was repeated at least three times with different cell preparations, and Figure 4, below, show representative experiments.

Results

In contrast to other eukaryotic cells, most of the calcium in different trypanosomatids such as *T. cruzi* (Docampo et al., 1995; Scott et al., 1997; Miranda et al., 2000), *T. brucei* (Vercesi et al., 1994; Scott et al., 1998; Rodrigues et al., 1999*a*), *Leishmania mexicana amazonensis* (Lu et al., 1997; Vannier-Santos et al., 1999) and *Leishmania donovani* (Rodrigues et al., 1999*b*) is concentrated in the acidocalcisomes. Acidocalcisomes have been morphologically defined in routine TEM preparations as empty vacuoles with a single membrane, circular shape, and electron-dense cores associated with the inner face of their membranes (Scott et al., 1997, 1998; Rodrigues et al., 1999*a*, 1999*b*; Miranda et al., 2000). This aspect as empty vacuoles is mainly attributed to the extraction of their mineral content during the conventional processing for transmission electron microscopy, which involves steps of fixation, dehydration, and embedding of the material (Miranda et al., 2000). When cryotechniques such as high-pressure freezing followed by freeze-substitution, cryosectioning followed by freeze-drying, or even when whole intact cell mounting techniques for TEM are applied, the acidocalcisomes appear as spherical electron-dense organelles with the whole matrix filled by an electron-dense material, which is mainly composed of oxygen, sodium, magnesium, phosphorus, potassium, calcium, and zinc as probed by energy-dispersive X-ray microanalysis (Scott et al., 1997; Miranda et al., 2000).

To investigate the presence of acidocalcisomes in *P. françai*, unfixed whole cells were air dried on formvar/carbon-coated TEM grids and observed in an energy-filtering TEM. This method was chosen to prevent and/or minimize the extraction of the mineral content of the acidocalcisomes during the routine TEM specimen preparation. Electron spectroscopic images showed a large number (208 ± 25) of dense organelles spread throughout the parasite cell without any preferential location (Fig. 1A). In contrast to the parasites thus far studied, the electron-dense organelles of *P. françai* were not all spherical. They appeared as pleomorphic structures with an elongated shape varying from 45 nm to 130 nm in width and 80 nm to 270 nm in length (Fig. 1B). Energy dispersive X-ray microanalysis showed considerable amounts of oxygen, sodium, magnesium, phosphorus, potassium, calcium, iron, and zinc in all

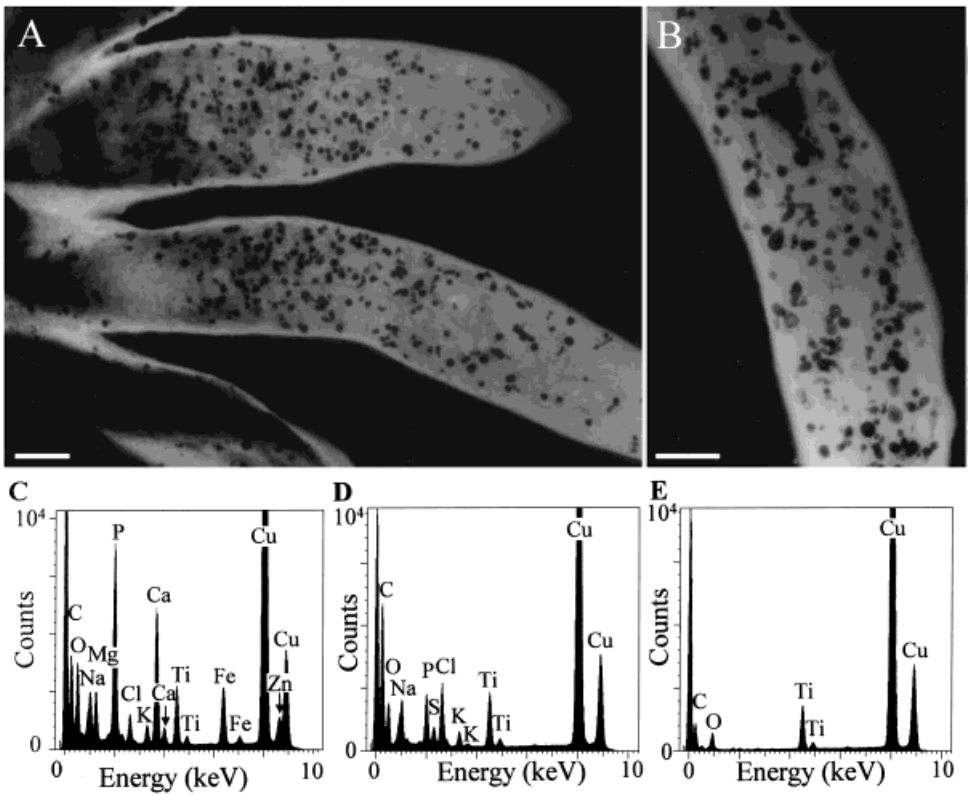

Figure 1. Presence of calcium-rich organelles in whole promastigotes. **A:** Electron spectroscopic image (ESI) of whole unstained cells showing numerous electron-dense organelles spread throughout the cell. **B:** High magnification showing the heterogeneity of shapes of dense organelles in *P. françai*. Note that some are almost spherical (arrows) whereas others appear as elongated structures (arrowheads). **C:** Typical X-ray spectrum of a dense organelle. Peaks of calcium, iron, phosphorus, sodium, magnesium, oxygen, carbon, and zinc, similar to that already described for the acidocalcisomes of different trypanosomatids (except for the presence of iron), can be observed. Occasionally potassium could also be found in some organelles. **D:** X-ray spectrum collected from a cytoplasmic region adjacent to the dense organelles. **E:** Control X-ray spectrum collected from the formvar/carbon film. Ti comes from the specimen holder and copper from the electron microscope grid. Bars: **A:** 1.3 μm; **B:** 1 μm.

dense organelles analyzed (Fig. 1C). X-ray microanalysis performed on different regions of the cytoplasm (Fig. 1D) and on fomvar/carbon film (Fig. 1E) did not show the calcium, iron, and zinc peaks characteristic of the electron dense organelles. Except for the presence of iron, the elemental composition of these organelles was similar to that found in acidocalcisomes of *T. cruzi* (Scott et al., 1997; Miranda et al., 2000), *T. brucei* (Rodrigues et al., 1999*a*), and *L. donovani* (Rodrigues et al., 1999*b*), thus providing evidence that, from the morphological point of view, the dense organelles of *P. françai* correspond to iron-rich acidocalcisomes. Elemental mapping showed that most of the magnesium, phosphorus, calcium, iron, and zinc is located within the acidocalcisomes (Fig. 2). In thin sections, these organelles appeared membrane limited, with the membrane surrounding electron-dense inclusions (Fig. 3A–G). As observed in whole cells, many vacuoles displayed an elongated shape (Fig. 3B,E,F). Some presented two or more inclusions (Fig. 3F) whereas others appeared completely filled, with the electron-dense material arranged in concentric patterns, suggesting the sequential deposition of material in the organellar matrix (Fig. 3E,G). Elongated structures resembling endoplasmic reticulum with an enlarged matrix also containing an electron-dense material were frequently seen (Fig. 3C). X-ray microanalysis confirmed that these organelles have the same composition as the dense organelles seen in whole-cell preparations (Fig. 3D).

Immunolocalization using polyclonal antibodies raised against a plant vacuolar proton pyrophosphatase showed a strong reaction with small intracellular structures in *P. françai* (Fig. 4A,B), indicating the presence of a H^+ PPase in these parasites. Cell fractionation performed using the iodixanol method, described before for the isolation of the acidocalcisomes of *T. cruzi* (Scott & Docampo, 2000), resulted in fractions in which it was possible to detect PP_i-driven H^+ uptake (Fig. 4C,D). Addition of PP_i was followed by a decrease in acridine orange absorbance, which was reversed by the addition of AMDP, a pyrophosphate analog which is known to specifically inhibit the H^+ pyrophosphatase, and by the K^+/H^+ ionophore nigericin (Fig. 4C). As

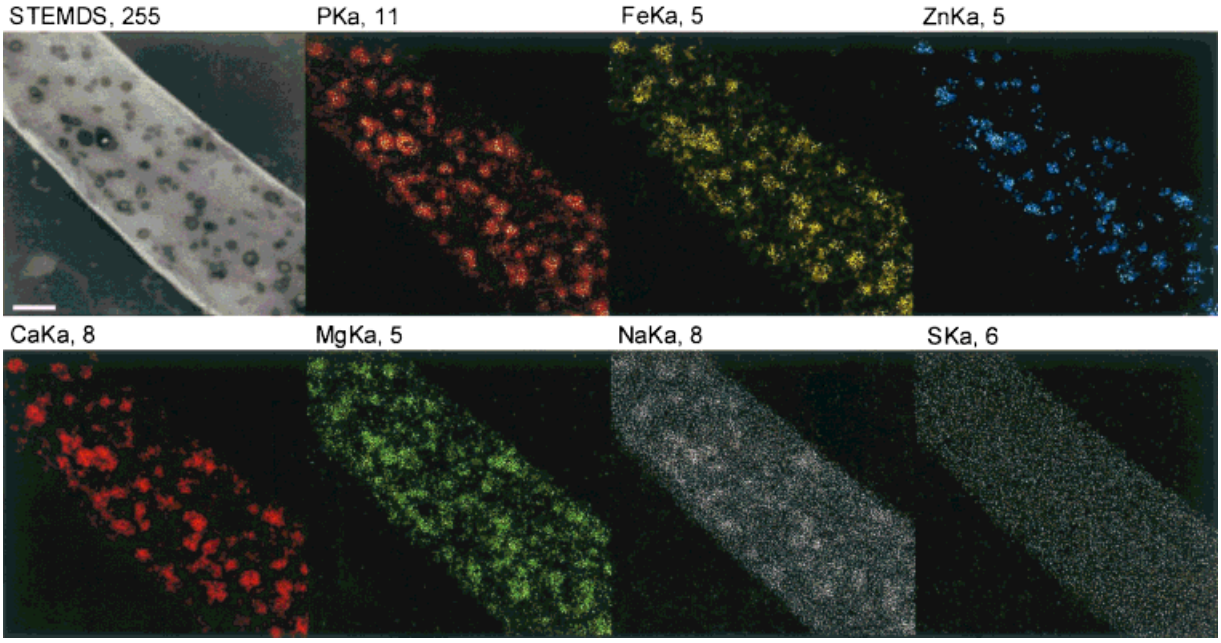

Figure 2. Elemental mapping of whole cells. Elemental mapping performed in whole cells shows that most of the calcium is localized within the acidocalcisomes comineralized with phosphorus, magnesium, sodium, iron, and zinc. Sulfur, although present, is not located within the acidocalcisomes. Bar: 1.1 μm.

shown in Figure 4D, the maximum activity was found in fraction 14 (bottom of the gradient). When this fraction was applied to formvar/carbon-coated electron microscope grids, it was shown to consist mainly of electron-dense organelles with the same morphology (Fig. 4E) and composition (Fig. 4F) as the dense organelles found in whole cells.

Discussion

Previous studies applying X-ray microanalysis and/or elemental mapping have reported the presence of iron-rich organelles in different trypanosomatids. *Trypanosoma cyclops* contains a prominent iron-containing vacuole only visible by light microscopy when cells are grown in the presence of hemoglobin, and for this reason they were thought to represent a phagosome or storage body containing haem derived from the incomplete digestion of hemoglobin (Vickerman & Tetley, 1977). *Herpetomonas samuelpessoai* also exhibit iron-rich electron-dense organelles similar to those found in *T. cyclops*, where iron may result from the degradation of hemin, an essential component of the culture media (Carvalho & de Souza, 1977). Elemental mapping of epimastigotes revealed substantial differences in the iron content in different strains of *T. cruzi* and in the color of the cell pellets (cells containing a high iron content displayed a brown color whereas cells with a low iron content displayed a white color; Dvorak et al., 1988). A subsequent quantitative work done in cryosections of *T. cruzi* identified two electron dense organelles in the epimastigote form (Scott et al., 1997). One was rich in calcium, phosphorus, and zinc but with no iron, thus corresponding to the acidocalcisome, and the other was calcium free, less electron dense if compared to acidocalcisomes, and contained high concentrations of iron and chloride. On the basis that epimastigotes are cultured in the presence of hemin and possess organelles of the endo-/lysosomal system (reservosomes) that are acidic and of similar size, the authors suggested that the iron-rich vesicles could correspond to the reservosomes (Scott et al., 1997). Accordingly, a later work where X-ray spectra were collected from reservosomes of epimastigotes that had incorporated gold-labeled albumin showed the presence of iron in these organelles (Miranda et al., 2000). Therefore, it is generally believed that the presence of iron in trypanosomatids is directly related to the degradation of incorporated iron-containing nutrients and growth factors (i.e., hemin, hemoglobin, and hematin) that are prelocalized in the newly formed endocytic compartments.

In *P. francai*, one remarkable characteristic of the acidocalcisomes is the presence of a high concentration of iron, a feature that, up to now, was unique to this parasite, except for its presence in acidocalcisomes of bloodstream forms of *T. cruzi* (Correa et al., 2002). Recent results from our laboratories have indicated that iron is also present in the acidocalcisomes of other members of the Trypanosomatidae family when cells are grown under similar conditions to those used to grow *P. francai* in this work (unpubl.

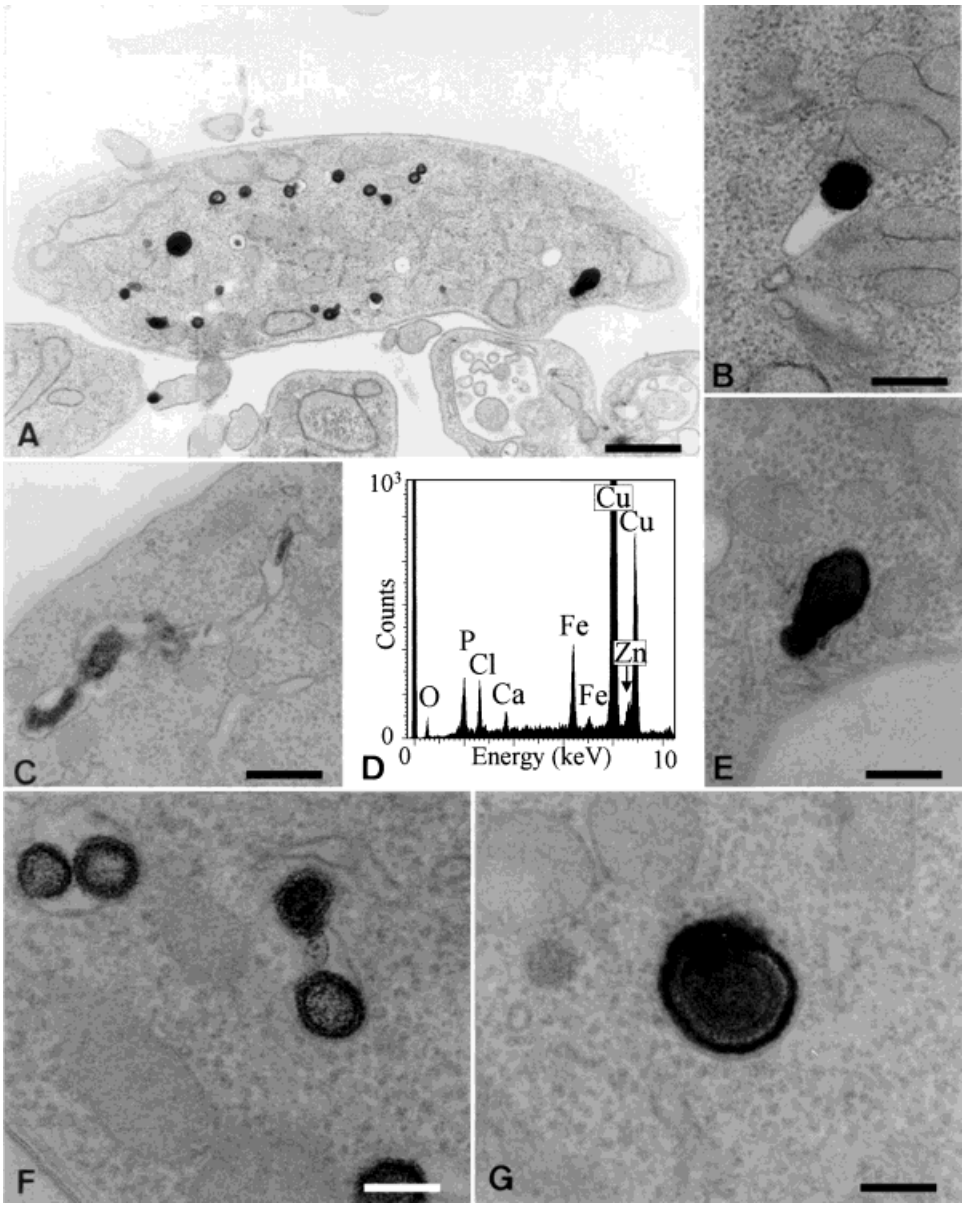

Figure 3. Electron-dense organelles of *P. françai* observed in thin section. **A:** Thin section of *P. françai* promastigote showing profiles of the electron dense organelles. **B**,**E:** High magnification showing organelles partially (**B**) or completely (**E**) filled with electron-dense material, which is rich in phosphate, calcium, iron, and zinc (**D**). Tubular structures, resembling enlarged endoplasmic reticulum, containing an electron dense material were also frequently seen (**C**). In some instances, two or more inclusions could be seen within these organelles (**F**). **G:** Organization of the electron-dense material in concentric patterns. Bars: **A:** 400 nm; **B:** 150 nm; **C:** 200 nm; **E:** 120 nm; **F:** 90 nm; **G:** 90 nm.

results). Acidocalcisomes of different parasites have been reported to contain a high concentration of pyrophosphate and polyphosphates together with magnesium, sodium, potassium, calcium, and zinc in their matrix (Docampo & Moreno, 1999, 2001). In spite of the fact that *P. françai* acidocalcisomes are rich in iron, several lines of evidence indicate that in many members of the Trypanosomatidae family these organelles do not belong to the endocytic pathway (reviewed in Docampo & Moreno, 2001). Polyphosphate bodies (acidocalcisomes) of procyclic trypomastigotes of *T. brucei* were shown to be inaccessible to horseradish peroxidase (Coppens et al., 1993), whereas loading of *T. cruzi* with gold-labeled transferrin (Scott et al., 1997) or albumin (Miranda et al., 2000) labeled the endo-/lysosomal system in the parasites but not the acidocalcisomes. In addition, cell fractionation studies using appropriate mark-

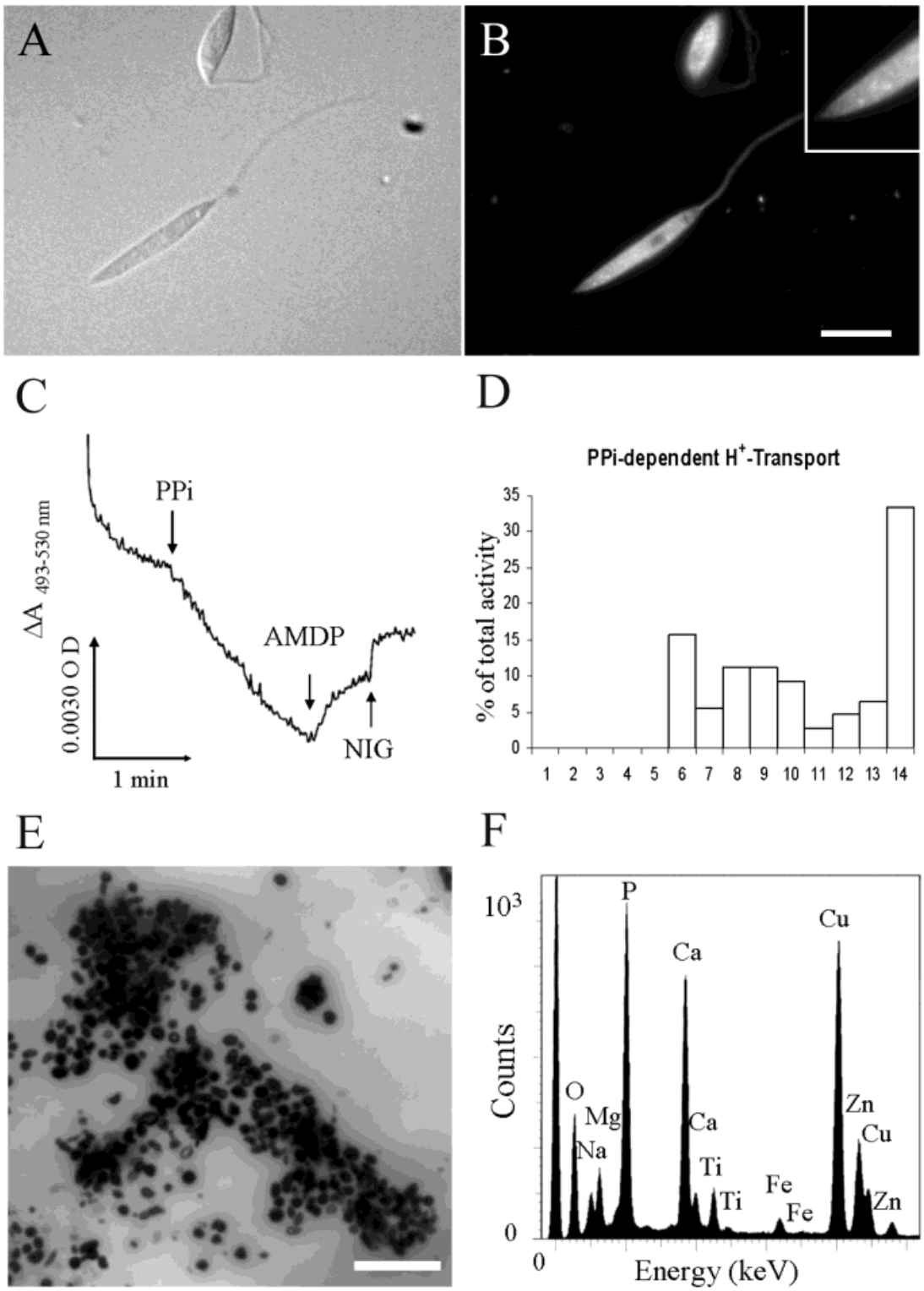

Figure 4. Presence of a vacuolar-type proton pyrophosphatase in the electron-dense organelles of *P. françai*. **A**,**B:** Immunofluorescence using antibodies raised against a plant V-type H^+-PPase. Images show cross-reaction of the antibody with small intracellular structures in a disposition similar to the acidocalcisomes observed in whole cells images. Bars: 7 μm. **C**,**D:** PPi-driven proton uptake in cell fractions. Fractions (0.1 mg/ml) were incubated in 130 mM KCl standard reaction medium containing in addition 1 μM oligomycin. Where indicated, 100 μM of sodium pyrophosphate (PPi), 20 μM aminomethylenediphosphonate (AMDP), and 1 μM nigericin (NIG) were added. Note that the highest activity was found in fraction 14 (**D**). **E:** Transmission electron micrograph of fraction 14 applied to a formvar/carbon-coated E.M. grid. Note that the fraction is enriched in electron-dense organelles. Bar: 700 nm. **F:** Energy dispersive X-ray spectrum showing the elemental profile of the isolated electron-dense organelles.

ers confirmed that these organelles are different from lysosomes and endocytic vacuoles (Scott et al., 1997; Rodrigues et al., 1999*a*, 1999*b*; Scott & Docampo, 2000). Many functions have been attributed to the acidocalcisome, from calcium uptake, storage, and signaling to polyphosphate storage and a potential role in the adaptation of the parasite to environmental stresses (Docampo & Moreno, 2001). Therefore, the finding of iron within the acidocalcisome matrix implies another important role for this organelle in the parasite's iron metabolism.

Iron constitutes an important element, being part of many molecules involved in several biological reactions, including oxygen transport, respiration, photosynthesis, and drug detoxification. However, iron is a toxic element, involved in a series of degradation processes such as the generation of reactive oxygen species, which damage a variety of biomolecules and disrupt the cell through interference in the structure of the lipid bilayer (Schmitt et al., 1993; Chou & Fitch, 1980). Therefore, as most of the iron is enclosed by the acidocalcisome membrane (as is apparent in the iron images; Fig. 2), the organelle could also play a role in a mechanism of iron detoxification by the parasite. It is possible that iron uptake into the acidocalcisomes occurs through an iron-transport system located in the acidocalcisome membrane. This transport system deserves further investigation.

The morphology of *P. françai* acidocalcisomes in thin sections is also an interesting point. The method applied in this preparation did not preserve the "native" structure of all the organelles but it seems that it favors the visualization of concentric patterns formed during the formation of the organelle, a feature that is completely different from other trypanosomatids so far studied (Docampo & Moreno, 1999, 2001). The degree of deposition and the mode of aggregation that occur in the organellar matrix may depend on a series of factors such as the internal pH of the organelle, composition of the matrix, rate of acquisition for each element, that is, the type and total activity for each transporter, channel, or exchanger, and on the metabolic requirements of the parasite. It is possible that in *P. françai* the aggregation of polyphosphates and cations in the acidocalcisomes occur in a different way from that supposed to lead to the formation of the microcrystalline aggregates in other trypanosomatids.

The cross-reaction of antibodies raised against the V-H^+-PPase with intracellular vesicles in the immunofluorescence experiments strongly suggested the presence of the enzyme in these parasites. Additionally, the detection of a V-H^+-PPase activity in cell fractions, especially in the fraction enriched of electron-dense organelles, indicates that in these parasites the enzyme is active. As the V-H^+-PPase has been found in the acidocalcisomes of a variety of parasites (Docampo & Moreno, 2001), and is therefore considered a marker for the organelle, the results support the idea that the iron-rich/calcium-containing organelles in *P. françai* correspond to acidocalcisomes.

In conclusion the results suggest that although acidocalcisomes of *P. françai* possess a proton-translocating pyrophosphatase they are morphologically slightly different from other acidocalcisomes described so far, and are rich in iron.

Acknowledgments

We thank Philip A. Rea for gifts of polyclonal antibodies and AMDP. This work was supported in part by grants from Conselho Nacional de Desenvolvimento Tecnológico-CNPq, Conselho de Aperfeiçoamento de Profissionais de Ensino Superior-CAPES, Fundação de Amparo a Pesquisa do Estado do Rio de Janeiro-FAPERJ, Fundação de Amparo a Pesquisa do Estado de São Paulo-FAPESP, Programa de Núcleos de Excelência-PRONEX and the National Institutes of Health (AI-23259 to R.D.).

References

Anonymous. (1997). Tropical Disease Research, Thirteenth Programme Report, UNDP/World Bank/World Health Organization Special Programme for Research and Training in Tropical Diseases. Geneva: World Health Organization.

Benaim, G. (1996). Intracellular calcium regulation and signaling in *Leishmania*. In *Molecular and Immune Mechanisms in the Pathogenesis of Cutaneous Leishmaniasis*, Tapia, F.J., Cáceres-Dittmar, G. & Sánchez, M.A. (Eds.), pp. 89–106. Georgetown, Texas: Landes Company.

Berridge, M.J. (1997). Elementary and global aspects of calcium signaling. *J Physiol* **499**, 291–306.

Camargo, E. (1999). *Phytomonas* and other Trypanosomatid parasites of plants and fruit. *Adv Parasitol* **42**, 29–112.

Carvalho, T.U. & de Souza, W. (1977). Fine structure and X-ray microanalysis of electron-dense granules in *Herpetomonas samuelpessoai*. *J Parasitol* **63**, 1116–1117.

Catarino, L.M., Serrano, M.G., Covazzana Jr., M., Almeida, M.L., Kaneshina, E.K., Campaner, M., Jankevicius, J.V., Teixeira, M.M.G. & Itow-Jankevicius, S. (2001). Classification of trypanosomatids from fruits and seed using morphological, biochemical and molecular markers revealed several genera amoung fruit isolates. *FEMS Microbiol Lett* **201**, 65–72.

Chou, A.C. & Fitch, C.D. (1980). Hemolysis of mouse erythrocytes by ferriprotoporphyrin IX and chloroquine. Chemotherapeutic implications. *J Clin Invest* **66**, 856–858.

Coppens, I., Baudhin, P., Opperdoes, F.R. & Courtoy, P.J. (1993). Role of acidic compartments in *Trypanosoma brucei*, with special reference to low density lipoprotein processing. *Mol Biochem Parasitol* **58**, 223–232.

Correa, A.F.S., Andrade, L.R. & Soares, M.J. (2002). Elemental composition of acidocalcisomes of *Trypanosoma cruzi* bloodstream trypomastigote forms. *Parasitol Res* **88**, 875–880.

Docampo, R. & Moreno, S.N.J. (1996). The role of Ca^{2+} in the process of cell invasion by intracellular parasites. *Parasitol Today* **12**, 61–65.

Docampo, R. & Moreno, S.N.J. (1999). Acidocalcisome: A novel Ca^{2+} storage compartment in trypanosomatids and apicomplexan parasites. *Parasitol Today* **15**, 443–448.

Docampo, R. & Moreno, S.N.J. (2001). The acidocalcisome. *Mol Biochem Parasitol* **33**, 151–159.

Docampo, R., Scott, D.A., Vercesi, A.E. & Moreno, S.N.J. (1995). Intracellular Ca^{2+} storage in acidocalcisomes of *Trypanosoma cruzi*. *Biochem J* **310**, 1005–1012.

Docampo, R. & Vercesi, A.E. (1989*a*). Ca^{2+} transport by coupled *Trypanosoma cruzi* mitochondria *in situ*. *J Biol Chem* **264**, 108–111.

Docampo, R. & Vercesi, A.E. (1989*b*). Characteristics of Ca^{2+} transport by *Trypanosoma cruzi* mitochondria *in situ*. *Arch Biochem Biophys* **272**, 122–129.

Dollet, M., Giannotti, J. & Ollagnier, M. (1977). Observation de protozoaires flagellés dans tubes cribles de palmiers à huile malades. *C R Acad Sci* **284**, 643–645.

Dvorak, J.A., Engel, J.C., Leapman, R.D., Swyt, C.R. & Pella, P.A. (1988). *Trypanosoma cruzi*: Elemental composition of cloned stocks. *Mol Biochem Parasitol* **31**, 19–26.

Kitajima, E.W., Vainstein, M.H. & Silveira, J.S.M. (1986). Flagellate protozoan associated with poor development of the root system of cassava in the Espirito Santo State, Brazil. *Phytopathology* **76**, 638–642.

Lafont, A. (1909). Sur la presence d'un *Leptomonas*, parasite de la classe des Flagellés, dans le latex de 'Euphorbia pilulifera. *C R Soc Seances Soc Biol Fil* **66**, 1011–1013.

Lu, H.-G., Zhong, L., Chang, K.P. & Docampo, R. (1997). Intracellular Ca^{2+} pool content and signaling and expression of a calcium pump are linked to virulence in *Leishmania mexicana amazonensis* amastigotes. *J Biol Chem* **272**, 9464–9673.

Miranda, K., Benchimol, M., Docampo, R. & De Souza, W. (2000). The fine structure of acidocalcisomes in *Trypanosoma cruzi*. *Parasitol Res* **86**, 373–384.

Moreno, S.N.J., Silva, J., Vercesi, A.E. & Docampo, R. (1994). Cytosolic-free calcium elevation in *Trypanosoma cruzi* is required for cell invasion. *J Exp Med* **180**, 1535–1540.

Parthasarathy, M.V., Van Slobbe, W.G. & Soudant, C. (1976). Trypanosomatid flagellate in the phloem of diseased coconut palms. *Science* **192**, 1346–1348.

Rodrigues, C.O., Scott, D.A. & Docampo, R. (1999*a*). Characterization of a vacuolar pyrophosphatase in *Trypanosoma brucei* and its localization to acidocalcisomes. *Mol Cell Biol* **19**, 7712–7723.

Rodrigues, C.O., Scott, D.A. & Docampo, R. (1999*b*). Presence of a vacuolar H^+-pyrophosphatase in promastigotes of *Leishmania donovani* and its localization to a different compartment from the vacuolar H^+-ATPase. *Biochem J* **340**, 759–766.

Schmitt, T.H., Frezzati, W.A. & Schreider, S. (1993). Hemin-induced lipid membrane disorder and increased permeability: A molecular model for the mechanism of cell lysis. *Arch Biochem Biophys* **307**, 96–103.

Scott, D.A., De Souza, W., Benchimol, M., Zhong, L., Lu, H.-G., Moreno, S.N.J. & Docampo, R. (1998). Presence of a plant-like proton-pumping pyrophosphatase in acidocalcisomes of *Trypanosoma cruzi*. *J Biol Chem* **273**, 22151–22158.

Scott, D.A. & Docampo, R. (2000). Characterization of isolated acidocalcisomes of *Trypanosoma cruzi*. *J Biol Chem* **275**, 24215–24221.

Scott, D.A., Docampo, R., Dvorak, J.A., Shi, S. & Leapman, R.D. (1997). *In situ* compositional analysis of acidocalcisomes in *Trypanosoma cruzi*. *J Biol Chem* **272**, 28020–28029.

Stahel, G. (1931). Zur kenntnis der siebroehrenkrankheit (Phloemnekrose) des kaffeebaumes in Surinam. I. Mikroskopische untersuchungen und infektionsversuche. *Phytopathol Zeitsch* **4**, 65–82.

Vainstein, M.H. & Roitman, I. (1985). Cultivation of *Phytomonas françai* associated with poor development of root of cassava. *J Protozool* **33**, 511–513.

Vannier-Santos, M.A., Martiny, A., Lins, U., Urbina, J.A., Borges, V.M. & De Souza, W. (1999). Impairment of sterol biosynthesis leads to phosphorous and calcium accumulation in *Leishmania* acidocalcisomes. *Microbiology* **145**, 3213–3220.

Vercesi, A.E., Bernardes, C.F., Hoffmann, M.E., Gadelha, F.R. & Docampo, R. (1991*a*). Digitonin permeabilization does not affect mitochondrial function and allows the determination of the mitochondrial membrane potential of *Trypanosoma cruzi in situ*. *J Biol Chem* **266**, 14431–14434.

Vercesi, A.E. & Docampo, R. (1996). Sodium-proton exchange stimulates Ca^{2+} release from acidocalcisomes of *Trypanosoma brucei*. *Biochem J* **315**, 265–270.

Vercesi, A.E., Grijalba, M. & Docampo, R. (1997). Inhibition of Ca^{2+} release from *Trypanosoma brucei* acidocalcisomes by 3,5-dibutyl-4-hydroxytoluene: Role of the Na^+/H^+ exchanger. *Biochem J* **328**, 479–482.

Vercesi, A.E., Hoffmann, M.E., Bernardes, C.F. & Docampo, R. (1991*b*). Regulation of intracellular calcium homeostasis in *Trypanosoma cruzi*. Effects of calmidazolium and trifluoperazine. *Cell Calcium* **12**, 361–369.

Vercesi, A.E., Moreno, S.N.J. & Docampo, R. (1994). Ca^{2+}/H^+ exchange in acidic vacuoles of *Trypanosoma brucei*. *Biochem J* **304**, 227–233.

Vercesi, A.E., Rodrigues, C.O., Catisti, R. & Docampo, R. (2000). Presence of a Na^+/H^+ exchanger in acidocalcisomes of *Leishmania donovani* and their alkalinization by ant-leishmanial drugs. *FEBS Lett* **473**, 203–206.

Vermeulen, H.A. (1963). A wilt *Coffea liberica* in Surinam and association with a flagellate, *Phytomonas leptovasorum*. *J Protozool* **10**, 216–222.

Vickerman, K. & Tetley, L. (1977). Recent ultrastructural studies on Trypanosomes. *Ann Soc Belge Med Trop* **57**, 441–455.

Vieira, M.C.F. & Moreno, S.N.J. (2000). Mobilization of intracellular calcium upon attachment of *Toxoplasma gondii* tachyzoites to human fibroblasts is required for invasion. *Mol Biochem Parasitol* **106**, 157–162.

Warren, L.G. (1960). Metabolism of *Schizotrypanum cruzi*. Chagas. I. Effect of culture age and substrate concentration on respiratory rate. *J Parasitol* **46**, 529–539.

Zhen, R.G., Baykov, A.A., Bakuleva, N.P. & Rea, P.A. (1994). Amynomethylenediphosphonate: A potent type-specific inhibitor of both plant and phototrophic bacterial H^+-pyrophosphatase. *Plant Physiol* **104**, 153–159.

Zhen, R.-G., Kim, E.J. & Rea, P.A. (1997). Acidic residues necessary for pyrophosphate-energized pumping and inhibition of the vacuolar H^+-pyrophosphatase by *N,N′*-diclyclohexylcarbodiimide. *J Biol Chem* **272**, 22340–22348.